IEEE Access
Multidisciplinary | Rapid Review | Open Access Journal

Received November 25, 2020, accepted December 11, 2020, date of publication December 14, 2020,
date of current version December 29, 2020.

Digital Object Identifier 10.1109/ACCESS.2020.3044699

Broadband Measurement of Substrate Complex Permittivity Using Optimized ABCD Matrix

LONGZHU CAI, (Member, IEEE), ZHI HAO JIANG, (Member, IEEE), AND WEI HONG, (Fellow, IEEE)

State Key Laboratory of Millimeter Waves, School of Information Science and Engineering, Southeast University, Nanjing 210096, China

Corresponding author: Longzhu Cai (longzhu.cai@seu.edu.cn)

This work was supported in part by the National Natural Science Foundation of China under Grant 61901108, in part by the Natural Science Foundation of Jiangsu Province, China, under Grant BK20180364, and in part by the National Key Research and Development Program of China under Grant 2019YFB2204704.

ABSTRACT In this paper, a novel two-transmission-line method based on optimized ABCD matrix for broadband and continuous substrate dielectric characterization is presented. The original single-line algorithm is firstly discussed and simulated, while the measurement shows that the extracted parameters are far from the actual values due to the presence of microwave connectors and transition mismatches. Therefore, a modified two-line algorithm based on the optimized ABCD matrix is proposed for ungrounded coplanar waveguide (UGCPW) configuration, which is very suitable for electroplating circuits with a consistent conductor layer on newly developed substrates. A comprehensive procedure to calculate the total line attenuation, phase number, characteristic impedance, substrate dielectric constant, and dielectric loss tangent is described. Since both conductor and radiation losses are taken into account, the extracted results show consistency within a single-digital percentage with the reference values. The analysis of the measurement uncertainty and the related uncertainty budgets for the derived dielectric results are also presented. The proposed method is expected to be applied to any transmission lines with arbitrary characteristic impedance, without a prior knowledge of substrate dielectric constant, and no additional calibrations are required other than the calibration kit for Vector Network Analyzer (VNA).

INDEX TERMS FR4 dielectric properties, complex permittivity, dielectric constant, dielectric loss tangent, microwave characterization, ABCD matrix.

I. INTRODUCTION

It is of vital necessity to know the dielectric properties (dielectric constant and dielectric loss tangent) of used substrates when microwave (MW) components and circuits are designed. With the material technology, more and more newly developed materials have been explored as dielectric substrates for applications in electromagnetic fields, such as textiles, epoxy films, cyclic olefin copolymer, etc. [1]–[7]. Thus, the extraction of dielectric properties in a wide band has always been significantly important and meaningful, particularly for newly developed materials.

A number of methods and techniques have been proposed in the literature for extracting dielectric properties of MW substrates, where the reported extraction techniques can be divided into narrowband measurement and wideband measurement according to bandwidth. The narrowband measurement technique is mainly based on resonant cavities, which can provide more accurate results, but only at discrete resonance points [8]–[10]. The wideband measurement technique primarily relies on the transmission/reflection of electromagnetic waves travelling through the material under test (MUT), hence the wideband measurement technique can provide a broadband and continuous material property [7].

One of the early attempts at implementing wideband measurement techniques was reported by Wan *et al.* to remove the error of two-port transmission parameter using wave cascading matrix (WCM) method in 1998, while this method is only suitable for characterizing well-matched devices [11]. Another early example was demonstrated in [12], where a two-line method was developed to measure substrate permittivity with the condition of relatively small coax-to-microstrip transition effect. It indicates that this technique requires a prior knowledge of an approximate substrate dielectric constant for 50-ohm characteristic impedance matching before measurement. On the other hand, an improved two-microstrip line (ML) technique was presented for a simple and accurate measurement of sub-

The associate editor coordinating the review of this manuscript and approving it for publication was Nosherwan Shoaib.

strate dielectric constant, without additional calibrations other than the 3.5-mm coaxial kit [13]. In a different example, a two-line method combined with matrix-pencil technique was described to remove the perturbation of effective dielectric constant due to the imperfect de-embedding and inhomogeneity of textiles with ML configurations [1].

In a more recent work, published in 2019, Ali *et al.* reported a WCM based multiline method to extract the dielectric properties of plastic filaments used for 3D printing [7]. The tested plastic filaments were placed inside the rectangular coaxial transmission-line fixtures, while the extraction error is extremely large due to the limitation of conductor loss in these fixtures. There are some other line-line methods for the extraction of dielectric substrate properties in literature. The study in [14] proposed a covered transmission-line method to determine substrate complex permittivity. Our previous work proposed a line-line method for characterizing dielectric parameters by utilizing the transmission coefficients [15]. In [16], a hybrid covered- and two-ML method for extracting dielectric properties was proposed. To sum up, the aforementioned multiline methods have more or less the following defects and deficiencies: some requiring a prior knowledge of dielectric constant for acceptable impedance matching and reflection; some only performing for the measurement of dielectric constant; some only operating under ML configurations; some only applying the transmission coefficient or WCM algorithm for derivation; some showing relatively low extraction accuracy.

Therefore, this paper proposes a two-transmission-line method based on an optimized ABCD matrix for characterizing dielectric materials with high extraction accuracy in a broad and continuous frequency band. The proposed method is expected to be applied to transmission lines with arbitrary characteristic impedance. In order to investigate the proposed extraction method, we choose ungrounded coplanar waveguide (UGCPW) transmission line as an example, which is well suited for electroplating circuits on newly developed dielectric materials, avoiding excessive fabrication cost and difficulty, as well as the problem and error of inconsistent conductor thickness and roughness caused by multiple electroplating steps. Compared to our previous work of characterizing dielectric parameters by utilizing the transmission coefficients [15], this study makes use of all scattering parameters ($S_{11}/S_{22}/S_{12}/S_{21}$) which are included in the expression of ABCD parameters, and it could provide more comprehensive and reliable extraction results. ABCD matrix is a link between the four scattering parameters and total line attenuation/phase number of transmission lines. Additionally, more parameters could be derived based on the proposed method, including the total line attenuation, phase number, characteristic impedance, substrate dielectric constant, and dielectric loss tangent, etc. To sum up, the novelty of this work mainly includes the following points:

1) We propose an optimized ABCD matrix for characterizing broadband and continuous substrate dielectric properties, and the original ABCD matrix is a link between the four scattering parameters and total line attenuation/phase number of transmission lines. The feasibility of the optimized ABCD matrix method is verified by the simulation and measurement of single-line/two-line algorithms.
2) The related multiline methods of deriving substrate dielectric properties in literature have more or less the following defects and deficiencies, such as requiring a prior knowledge of dielectric constant for acceptable impedance matching and reflection, only operating under microstrip line configurations, applying transmission coefficient or WCM algorithm, owing low extraction accuracy, etc. While our proposed method does not have these issues, and possesses new calculation techniques.
3) We choose ungrounded coplanar waveguide (UGCPW) transmission line as an example to verify the proposed method. UGCPW is very suitable for parameter extraction of newly developed dielectric substrates, as it is easier to obtain consistent conductive layer, avoiding excessive fabrication cost and difficulty, as well as the problem and error of inconsistent conductor thickness and roughness caused by multiple electroplating steps.
4) The proposed method could be applied to other transmission lines with arbitrary characteristic impedance without a prior knowledge of substrate dielectric constant, and no additional calibrations are required other than the calibration kit for Vector Network Analyzer (VNA). More parameters could be derived based on the proposed method, including the total line attenuation, phase number, characteristic impedance, substrate dielectric constant, and dielectric loss tangent, etc., and radiation loss is included in the calculation to ensure the extraction accuracy. The measurement uncertainty analysis and the uncertainty budgets at selected frequencies are also presented.

This paper is organized as follows. In section II, the theory analysis and simulation validation of single-line algorithm are presented, including the calculation of line attenuation and phase number based on ABCD matrix, the dielectric constant and dielectric loss tangent obtained by further extraction, as well as the simulation verification based on UGCPW structure. In section III, the optimized two-line algorithm based on the modified ABCD matrix is described in detail, where the experimental results of the extracted dielectric properties according to the single-line and two-line algorithms are presented for verification, as well as the measurement uncertainty analysis. Conclusions are provided in Section IV.

II. SIMULATION VALIDATION OF SINGLE-LINE ALGORITHM

In order to characterize a two-port network, the equation containing ABCD matrix can be expressed as follows [17]

$$\begin{bmatrix} V_1 \\ I_1 \end{bmatrix} = \begin{bmatrix} A & B \\ C & D \end{bmatrix} \begin{bmatrix} V_2 \\ -I_2 \end{bmatrix}, \tag{1}$$

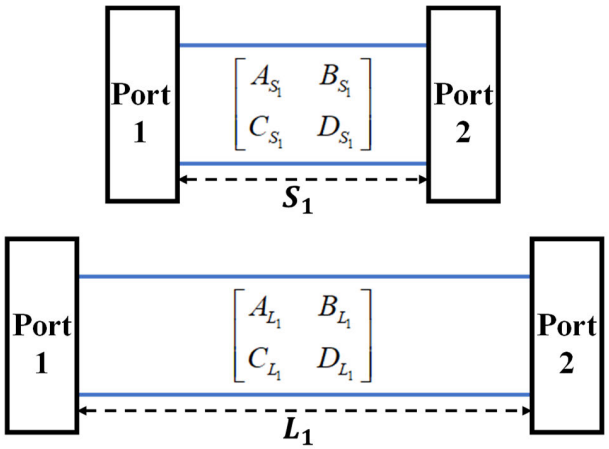

FIGURE 1. Test fixture schematic for two-port transmission lines represented by ABCD matrix with length S_1 and L_1 ($L_1 > S_1$).

where the matrix made of ABCD parameters is defined as ABCD matrix, and V_1, V_2, and I_1, I_2 are the voltage and current variables at port 1 and port 2, respectively. Fig. 1 exhibits a simple test fixture schematic for two-port transmission lines represented by ABCD matrix with length S_1 and $L_1 (L_1 > S_1)$. For a transmission line with length l and characteristic impedance Z_c, the values of ABCD parameters can be calculated by formula (2) [17], and $\gamma = \alpha + j\beta$ is the complex propagation constant.

$$A = \cosh \gamma l \quad B = Z_c \sinh \gamma l$$
$$C = \frac{\sinh \gamma l}{Z_c} \quad D = \cosh \gamma l, \tag{2}$$

Equation (3) describes the conversion relationship between the S-parameters and ABCD parameters [17]. By combining Equations (2) and (3), the line attenuation α and phase number β can be derived in terms of ABCD parameters (Equation (4) and (5)), and they are tightly correlated with scattering parameters (S-parameters) that can be obtained directly from vector network analyzers (VNA) [17]. Note that α and β own the units of dB/m and rad/m, respectively.

$$\begin{bmatrix} A & B \\ C & D \end{bmatrix} = \begin{bmatrix} \frac{(1+S_{11})(1-S_{22})+S_{12}S_{21}}{2S_{21}} & Z_c \frac{(1+S_{11})(1+S_{22})-S_{12}S_{21}}{2S_{21}} \\ \frac{1}{Z_c} \frac{(1-S_{11})(1-S_{22})-S_{12}S_{21}}{2S_{21}} & \frac{(1-S_{11})(1+S_{22})+S_{12}S_{21}}{2S_{21}} \end{bmatrix}, \tag{3}$$

$$\alpha = \frac{1}{l} \frac{20}{\ln 10} Re \left\{ \ln \left[\frac{(A+D) \pm \sqrt{(A+D)^2 - 4}}{2} \right] \right\} \text{ (dB/m)}, \tag{4}$$

$$\beta = \frac{1}{l} \text{Im} \left\{ \ln \left[\frac{(A+D) \pm \sqrt{(A+D)^2 - 4}}{2} \right] \right\} = \frac{2\pi f \sqrt{\varepsilon_{eff}}}{c} \text{ (rad/m)}. \tag{5}$$

Based on the equation (5), the effective dielectric constant ε_{eff} can be derived, which leads to the extraction of substrate dielectric constant ε_r by using [18]

$$\varepsilon_r = 1 + \frac{\varepsilon_{eff} - 1}{q}, \tag{6}$$

where q is the filling factor that is mainly determined by the type of the used transmission line and its physical dimensions. The substrate dielectric loss tangent $\tan \delta$ is correlated with its dielectric loss α_d, which can be calculated according to equations (7) and (8) below, where α_c and α_r are the conductor loss and radiation loss, respectively [18].

$$\alpha_d = \alpha - \alpha_c - \alpha_r, \tag{7}$$

$$\tan \delta = \frac{\alpha_d c \sqrt{\varepsilon_{eff}}}{q \varepsilon_r f \pi} \frac{1}{\frac{20}{\ln 10}}. \tag{8}$$

UGCPW straight transmission lines are used as an example to investigate the proposed algorithm. As described in [15], it is very suitable to use the UGCPW structure for electroplating circuit on newly developed dielectric materials, avoiding excessive fabrication cost and difficulty, as well as the problem and error of inconsistent conductor thickness and roughness caused by multiple electroplating steps. High Frequency Structural Simulator (HFSS) software is employed for theoretical simulation and calculation. Two wave ports are applied in simulation on both sides of UGCPW straight lines based on the proposed MUT-FR4 substrate. The single-line algorithm is firstly evaluated with a UGCPW line with length l. The obtained S-parameters could be converted into ABCD parameters by equation (3). Then the total phase can be calculated with the unit of rad according to formula (5). Fig. 2(a) shows its original wrapped positive value, which is then transformed into a set of data with positive and negative values depicted as processed total phase in the figure, and it actually alternate between $-\pi$ and π. Note that the unit of the phase in Fig. 2(a) is in rad instead of rad/m. The processed total phase can be further unwrapped and linearized, then divided by length l to get the phase number β in the unit of rad/m. It can be seen from formula (5) that the phase number β and its working frequency f are in a linear relationship, which is presented in Fig. 2(b). Once the phase number β is known, the effective dielectric constant ε_{eff} and substrate dielectric constant ε_r can be extracted from equation (5) and (6), respectively, which are also shown in Fig. 2(b). It is noticeable that, in the frequency range of 5–20 GHz, the derived ε_{eff} and ε_r are very smooth and stable, which are maintained at around 2.28 and 4.42, respectively. The derived dielectric constant is remarkably consistent with the reference value 4.4, showing only 0.02 (0.45%) difference at 10 GHz.

The line attenuation α can be obtained according to equation (4). In order to acquire the dielectric loss α_d (see equation (7)), the corresponding radiation loss α_r and conductor loss α_c also need to be calculated. For UGCPW straight transmission line structures, the radiation loss α_r is very small, which can be roughly described by equation (9) [15], [19]. In equation (9), $f(\varepsilon_r)$ and λ_d are the radiation form factor and dielectric wavelength, respectively. The conductor loss α_c of UGCPW straight transmission lines can be expressed as equation (10), which is related to the characteristic impedance Z_c, the distributed series resistance of center strip conductor R_c, and the distributed series resistance of the ground planes

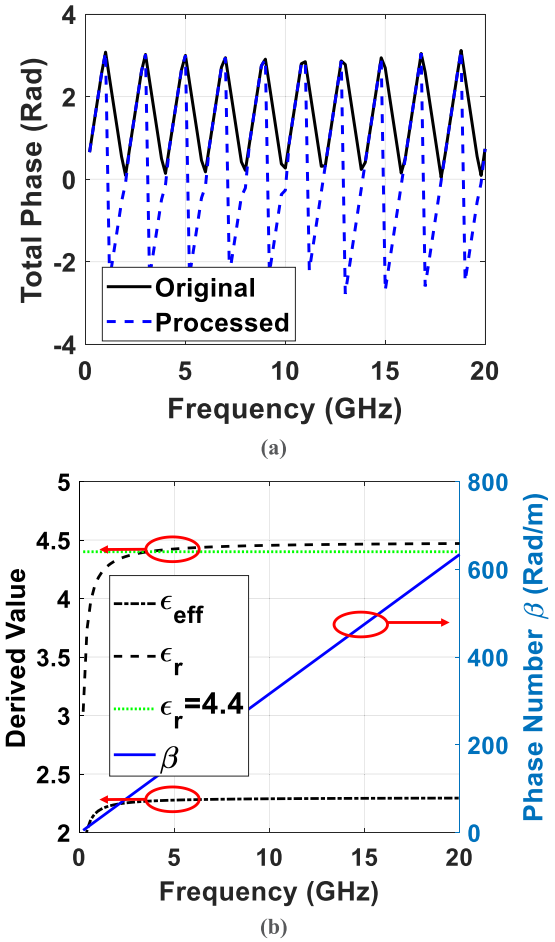

FIGURE 2. (a) The original wrapped total phase and the processed total phase. (b) The derived phase number β in Rad/m, the effective dielectric constant ε_{eff}, and the dielectric constant ε_r for the proposed structure.

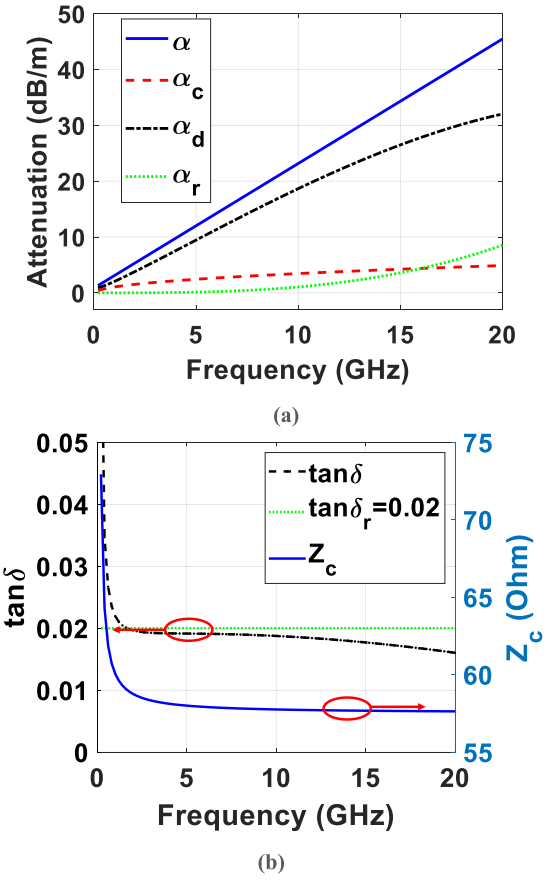

FIGURE 3. (a) The derived total line attenuation (α) and the parts from conductor (α_c), dielectric (α_d), and radiation (α_r). (b) The derived dielectric loss tangent tan δ and characteristic impedance Z_c.

R_g [15]. The characteristic impedance Z_c could be determined by the effective dielectric constant ε_{eff} and the complete elliptic integral of the first kind K, which is associated with UGCPW structure dimensions, including the signal line width S, gap W, and substrate thickness H. The expression of characteristic impedance Z_c is given in equation (11). The derivation details of equation (9)–(11) can be found in [15], [19], [20].

$$\alpha_r = f(\varepsilon_r)\left(\frac{1}{\lambda_d}\right)^3 \frac{(S+2W)^2}{K(k_0)K'(k_0)}, \tag{9}$$

$$\alpha_c = \frac{20}{\ln 10}\frac{R_c + R_g}{2Z_c}, \tag{10}$$

$$Z_c = \frac{30\pi}{\sqrt{\varepsilon_{eff}(f)}\left(\frac{K(k_0)}{K(k_0')}\right)}, \tag{11}$$

Fig. 3(a) shows the value of total attenuation α, conductor loss α_c, radiation loss α_r, and dielectric loss α_d of the proposed UGCPW model. From equation (8) the dielectric loss tangent tan δ can be derived, which is presented in Fig. 3(b). We can see that the calculated tan δ matches very well with the reference value 0.02 in a wide frequency band of 2–20 GHz. The derived dielectric loss tangent at 2 GHz, 5 GHz, 10 GHz, 15 GHz, and 20 GHz are 0.0196, 0.0191, 0.0188, 0.018, and 0.0168, respectively. It indicates that the corresponding deviations compared with the reference value at these frequencies are 0.0004 (2%), 0.0009 (4.5%), 0.0012 (6%), 0.002 (10%), and 0.0032 (16%), respectively. Moreover, the derived characteristic impedance Z_c across the frequency range is $\sim$ 58Ω, which indicates that we can still acquire substrate dielectric parameters with high accuracy under the condition of unknown dielectric constant and unmatched structure. The simulation results verify the validity and feasibility of the single-line algorithm.

III. THE OPTIMIZED TWO-LINE ALGORITHM AND EXPERIMENTAL RESULTS

In order to verify the single-line algorithm in experiment, we fabricated two UGCPW straight lines with the same mechanical dimension except various length. For better verification and comparison, the devices used in this method are the same as those in [15], and the specific device dimensions can be found in Section III of [15]. Full two-port calibration was performed using 2.4-mm calibration kit for VNA N5247A, where transmission lines with embedded SMA connectors are then connected. Fig. 4 shows the measurement setup with the fabricated short UGCPW straight line. Measurement shows that the extracted results based on the long and short lines are inconsistent, both of which are far from the actual values, and the related results are shown in Fig. 5. The results based on a new and optimized two-line

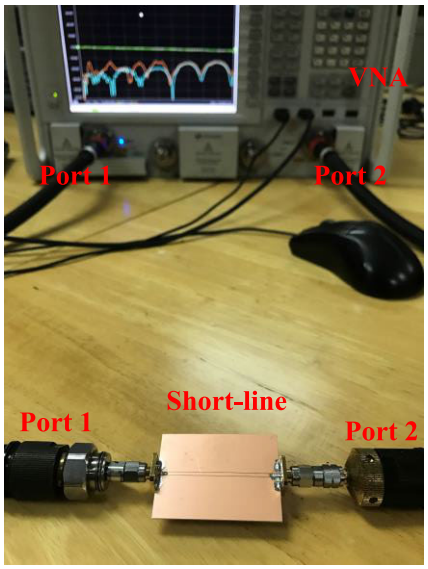

FIGURE 4. Measurement setup with the fabricated short UGCPW straight line.

algorithm are also presented in this figure. The following will introduce the proposed two-line algorithm.

For long and short transmission lines with length L_1 and S_1 (see Fig. 1), the measured S-parameters can be converted into ABCD parameters based on equation (3).

$$[Measured\ S\ parameters] \Rightarrow \begin{bmatrix} A_{L_1} & B_{L_1} \\ C_{L_1} & D_{L_1} \end{bmatrix},\ for\ long-line\ L_1.$$

$$[Measured\ S\ parameters] \Rightarrow \begin{bmatrix} A_{S_1} & B_{S_1} \\ C_{S_1} & D_{S_1} \end{bmatrix},\ for\ short-line\ S_1.$$

Therefore, the phase number β based on the optimized two-line algorithm is expressed in equation (12). The effective dielectric constant ε_{eff} and dielectric constant ε_r could be further extracted according to equation (12) and (6). Fig. 5 depicts the derived phase number β, effective dielectric constant ε_{eff} and dielectric constant ε_r, based on the one-line algorithm (long-line and short line) and two-line algorithm.

$$\begin{aligned}\beta &= \frac{1}{L_1 - S_1}\mathrm{Im}\left\{\ln\left[\frac{(A_{L_1} + D_{L_1}) \pm \sqrt{(A_{L_1} + D_{L_1})^2 - 4}}{2}\right]\right. \\ &\quad \left. - \ln\left[\frac{(A_{S_1} + D_{S_1}) \pm \sqrt{(A_{S_1} + D_{S_1})^2 - 4}}{2}\right]\right\} \\ &= \frac{2\pi f\sqrt{\varepsilon_{eff}}}{c}(\mathrm{rad/m}) \qquad (12)\end{aligned}$$

As can be seen form Fig. 5(c), the extracted ε_r at 10 GHz are 17.37, 9.95, and 4.37, respectively, for the short-line, long-line, and two-line based algorithms. Since at 10 GHz the ε_r and $\tan\delta$ of the MUT provided by the vendor are 4.4 and 0.02, respectively, it clearly shows that the extracted ε_r based on the optimized two-line algorithm is closer to the reference value, with a difference of only ∼0.03 (0.68%) to ∼0.07 (1.59%) in an extremely wide frequency band (4 to 20 GHz). The transitions and connections between MW connectors and transmission lines were not included in the theoretical analysis of the single-line algorithm shown in section II, while in measurement SMA connectors inevitably introduce

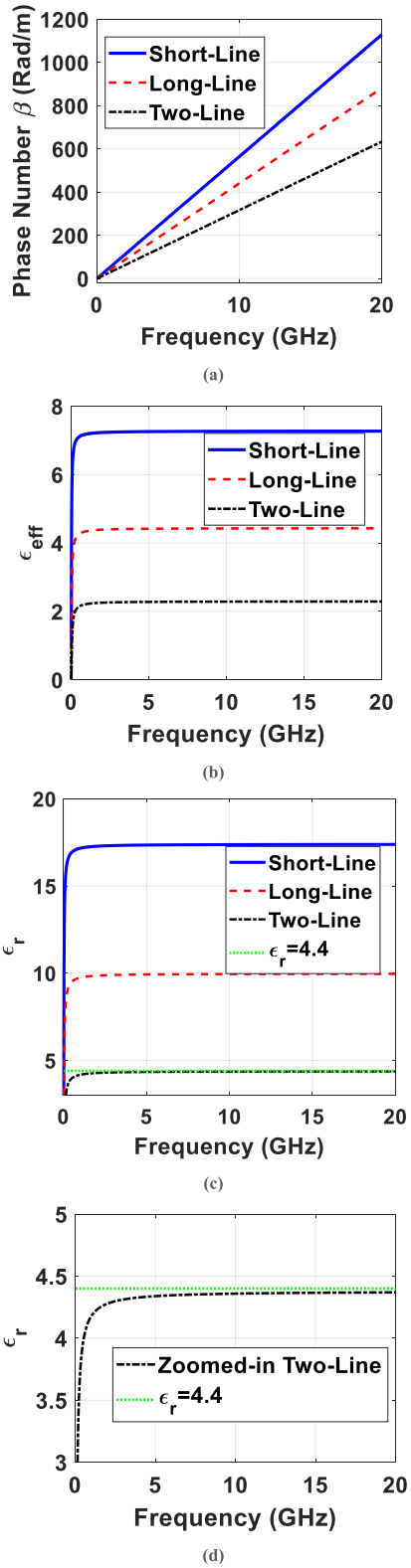

FIGURE 5. (a) The derived phase number β, (b) effective dielectric constant ε_{eff}, (c) dielectric constant ε_r, based on the one-line and two-line algorithms, (d) zoomed-in dielectric constant ε_r based on the two-line algorithm.

a change of the obtained S-parameters, which leads to very large extraction error of the single-line algorithm in the actual test. The extracted ε_r based on the long and short transmission lines are not the same due to different influences on the lines,

both of which are far from the provided reference value. For the optimized two-line algorithm, the error caused by the transition and connection can be alleviated by comparing the measured S-parameters of these two lines, which leads to high extraction accuracy, so the two-line algorithm is more suitable for practical applications. Since welding influence part accounts for a larger proportion of short-line length when comparing with long-line length, the transition would have a greater impact on the short line, which is the reason why the extracted dielectric constant based on the short line deviates more from the reference value (see Fig. 5c).

The line attenuation based on the two-line algorithm can be written as

$$\alpha = \frac{1}{L_1 - S_1}\frac{20}{\ln 10} \times \mathrm{Re}\left\{ \begin{array}{l} \ln\left[\frac{(A_{L_1}+D_{L_1}) \pm \sqrt{(A_{L_1}+D_{L_1})^2-4}}{2}\right] \\ -\ln\left[\frac{(A_{S_1}+D_{S_1}) \pm \sqrt{(A_{S_1}+D_{S_1})^2-4}}{2}\right] \end{array} \right\} \text{(dB/m)} \quad (13)$$

which assumes that the transition and connection between the MW connectors and the two transmission lines are completely identical, so as to mitigate the extraction error. Fig. 6(a) shows the extracted overall line attenuation α based on the proposed two-line algorithm, as well as conductor loss α_c, radiation loss α_r, and dielectric loss α_d. It can be seen from the figure that the dielectric loss accounts for the great majority of the overall line attenuation for the selected MUT-based UGCPW configuration, the results of which are very similar to that of the previous work by applying the transmission coefficient [15]. The dielectric loss tangent $\tan\delta$ can be derived according to equation (8), as depicted in Fig. 6(b), indicating that the dielectric loss tangent gradually increases from 0.0186 to 0.0214 between 8 and 20 GHz, with a difference of 0.0014 (7%) when compared with the reference (0.02). Moreover, the reference value 0.02 provided by the vendor is for 10 GHz, while the extracted $\tan\delta$ at 10 GHz is 0.0199, with a slight discrepancy of 0.0001 (0.5%). The extraction accuracy below 8 GHz becomes relatively poor. This is due to the fact that the corresponding electric lengths of the lines are too small at low frequencies. The results above 20 GHz are not provided in this work due to the upper frequency limit of the applied SMA connectors. The accuracy of the derived ε_r and $\tan\delta$ at 10 GHz based on the proposed two-line algorithm are 0.68% (4.37 vs 4.4) and 0.5% (0.0199 vs 0.02), respectively. The extraction accuracy of the proposed method is higher than that of our previous work using transmission coefficient, as well as other single-line or multiline methods based on covered or WCM ML algorithms [1], [7], [14]–[16], [21]. For instance, the extraction errors of $\varepsilon_r/\tan\delta$ presented in the literature [14] [16] are 0.03/0.0015 and 0.01/0.0004, respectively. Table 1 summarizes the comparison between the proposed extraction method

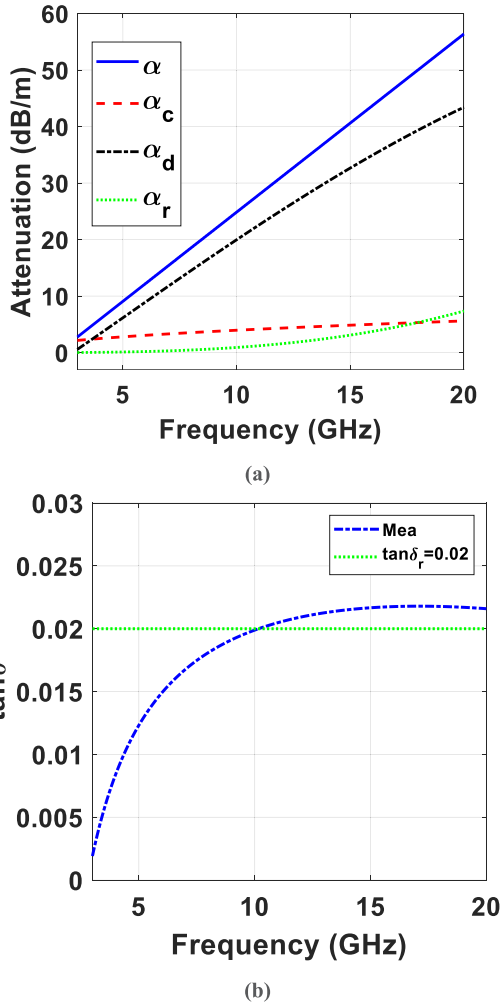

FIGURE 6. The extracted (a) overall line attenuation α, conductor loss α_c, radiation loss α_r, and dielectric loss α_d, and (b) dielectric loss tangent, based on the proposed two-line algorithm.

and some reported ones in literature for Substrate Complex Permittivity Measurement.

There are several sources of error and uncertainty in the measurement of dielectric characterization, mainly including the fabrication tolerance and the VNA measurement error [23]–[26]. Firstly, one of the main sources of error and uncertainty comes from the fabrication tolerance. Based on the proposed UGCPW structure and deriving technique, the fabrication tolerance may consist of four parts, which are the transmission line length l, the signal line width S, the gap W, and the dielectric substrate thickness H. Considering that the largest dimension tolerance is 1 mil (0.0254 mm), the dimensions of the above four parameters might be 1 mil larger (+1 mil) or smaller (−1 mil). Through the proposed algorithm, the updated dielectric constant and dielectric loss tangent at different parameter dimensions and frequencies are depicted in Fig. 7. The labelled *max* and *min* in the figure represent the corresponding results when parameters become larger (+1 mil) and smaller (−1 mil), respectively. It is worth mentioning that *E_L_max* and *E_L_min* have considered the cases of the combination of longer line

TABLE 1. Comparison of selected methods for substrate complex permittivity measurement.

Ref.	TL type/Method	Ref. MUT	Frequency Range (GHz)	$\Delta\varepsilon$	$\Delta \tan\delta$
[8]	ML /Resonator	FR4	0.5-10.5 (Discrete)	~0.07 (1.7%)	~0.003 (15%)
[22]	ML /Resonator	FR4	2-12 (Discrete)	~0.06 (1.5%)	NA
[21]	ML /Single-line	Rogers RO3850/ RO3006/ RO3010	To 67	~0.1-0.5 (3%-8%)	~0.004 -0.008 (100%-200%)
[7]	Coaxial TL/Two-line+WCM	3D printing materials	To 10	5%	10%
[1]	ML/Two-line+WCM	RT/d 5870	To 10	0.03 (1.3%)	NA
[14]	ML/Covered ML	RT/d 5880	59-61	0.03	0.0015
[15]	UGCPW/Two-line+Transmission	FR4	to 20	~0.03 (0.68%)	~0.0013 (6.5%)
[16]	ML/Hybrid covered+two-line	RT/d 5880	37-39	0.01 (0.45%)	0.0004 (44.4%)
This work	UGCPW/Two-line+ ABCD matrix	FR4	to 20	**~0.03 (0.68 %)**	**~0.0001 (0.5%)**

becoming longer (+1 mil) and shorter line becoming shorter (−1 mil), and the combination of longer line becoming shorter (−1 mil) and shorter line becoming longer (+1 mil). It can be observed from the figure that the gap W and substrate thickness H have greater influence on ε_r than that of the transmission line length l and width S. The maximum uncertainty caused by W and H on ε_r is ~ 0.058 ($\sim 1.34\%$) in the frequency range of 5–20 GHz, while that caused by l and S is ~ 0.0122 ($\sim 0.28\%$) and ~ 0.0144 ($\sim 0.33\%$), respectively. In addition, the uncertainty relying on the gap W has the most significant influence on $tan\delta$. At 10 GHz, the maximum uncertainty caused by W, l, S, and H on $\tan\delta$ is $\sim 4.33\times10^{-4}$ ($\sim 2.18\%$), $\sim 1.96\times10^{-5}$ ($\sim 0.099\%$), $\sim 5.97\times10^{-6}$ ($\sim 0.03\%$), and $\sim 5.13\times10^{-5}$ ($\sim 0.26\%$), respectively. These uncertainty contributions are squared summed and re-rooted to form the combined standard uncertainty. Eventually, the combined standard uncertainty of ε_r and $\tan\delta$ due to the effect of fabrication tolerance at 10 GHz are ~ 0.084 ($\sim 1.93\%$) and $\sim 4.37\times10^{-4}$ ($\sim 2.20\%$), respectively.

Another source of error and uncertainty is from VNA measurement system, and it can be estimated by a variety of models, among which *Metas.UncLib* is a commonly used method [26]–[28]. *Metas.UncLib* applies differentiation techniques and tracks the dependence of error terms in measurement model, which is described in [27]. Generally, the VNA

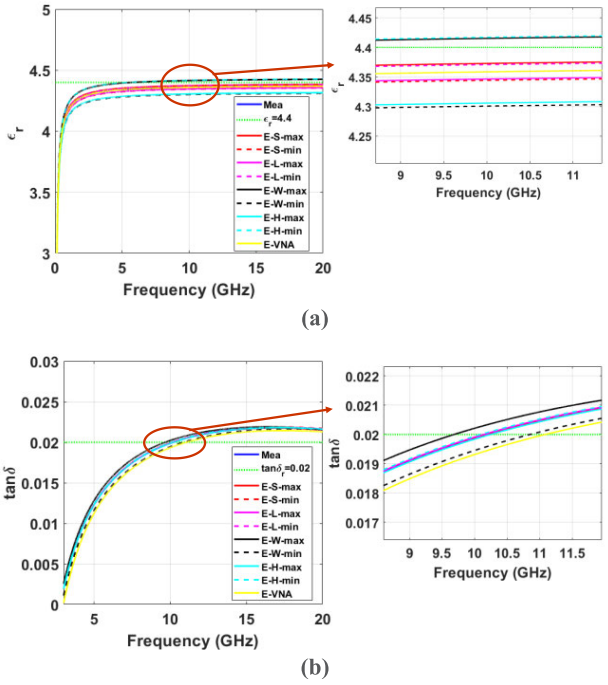

FIGURE 7. Uncertainty sensitivity of (a) dielectric constant ε_r and (b) dielectric loss tangent $tan\delta$ due to the fabrication tolerance and VNA measurement error (E_VNA). Fabrication tolerance comes from the transmission line length *l* (E_L_max and E_L_min), the signal line width *S* (E_S_max and E_S_min), the gap *W* (E_W_max and E_W_min), and the dielectric substrate thickness *H* (E_H_max and E_H_min). Noting that Max and Min represent the cases when these parameters become 1 mil larger and smaller, respectively.

measurement uncertainty is related to the following terms, including VNA noise, linearity, drift, cable stability, and connector repeatability, all of which could contribute to the overall measurement uncertainty of S-parameters. Given nominal magnitude error of S-parameters approximately 0.015 due to VNA measurement uncertainty [23], the associated ε_r and $\tan\delta$ at different frequencies can be obtained, which is shown in Fig. 7 (labelled as E_VNA). In this case, the influence of VNA measurement error on ε_r remains almost unchanged, while it has a large impact on $\tan\delta$, and the derived uncertainty at 10 GHz is $\sim 5.73\times10^{-4}$ ($\sim 2.88\%$). The uncertainty budgets showing the main uncertainty contributions for ε_r and $\tan\delta$ at 5/10/15/20 GHz are presented in Table 2 and 3. It can be observed from the results that the combined total standard uncertainty in our proposed technique is smaller than that of the recently published work, where the estimated uncertainty of ε_r and $\tan\delta$ in the transmission-only method is $3\% - 4\%$ and $10\% - 15\%$, respectively [23].

For the proposed two-line algorithm, it assumes that the transition and connection between MW connectors and transmission lines are mechanically and electrically identical, while in practical cases they are not likely to be completely the same. More advanced welding and connection techniques could make the welding and connection of these lines more identical and closer, which would expand the applicability of the proposed method and increase the accuracy of extracted parameters. In addition, multiple transmission lines

TABLE 2. Uncertainty budget ($\Delta\varepsilon_r$) for the dielectric constant due to the fabrication tolerance and VNA measurement error.

Para.	5 GHz	10 GHz	15 GHz	20 GHz
S	0.0143 (0.33%)	0.0144 (0.33%)	0.0144 (0.33%)	0.0144 (0.33%)
l	0.0121 (0.28%)	0.0122 (0.28%)	0.0122 (0.28%)	0.0122 (0.28%)
W	0.0575 (1.32%)	0.0578 (1.33%)	0.0579 (1.33%)	0.0580 (1.33%)
H	0.0581 (1.34%)	0.0584 (1.34%)	0.0585 (1.34%)	0.0586 (1.34%)
VNA	1.57×10^{-5} (~0)	5.47×10^{-7} (~0)	5.99×10^{-6} (~0)	8.71×10^{-6} (~0)
Total	0.0838 (1.93%)	0.0843 (1.93%)	0.0845 (1.94%)	0.0846 (1.94%)

TABLE 3. Uncertainty budget ($\Delta\tan\delta$) for the dielectric loss tangent due to the fabrication tolerance and vna measurement error.

Para.	5 GHz	10 GHz	15 GHz	20 GHz
S	3.22×10^{-5} (0.26%)	5.97×10^{-6} (0.03%)	4.08×10^{-5} (0.19%)	1.04×10^{-4} (0.48%)
l	1.05×10^{-5} (0.085%)	1.96×10^{-5} (0.099%)	2.67×10^{-5} (0.12%)	3.48×10^{-5} (0.16%)
W	6.56×10^{-4} (5.33%)	4.33×10^{-4} (2.18%)	2.45×10^{-4} (1.13%)	5.43×10^{-5} (0.25%)
H	4.20×10^{-5} (0.34%)	5.13×10^{-5} (0.26%)	2.49×10^{-5} (0.11%)	2.36×10^{-5} (0.11%)
VNA	1.10×10^{-3} (8.72%)	5.73×10^{-4} (2.88%)	4.06×10^{-4} (1.88%)	3.23×10^{-4} (1.5%)
Total	1.30×10^{-3} (10.23%)	7.2×10^{-4} (3.62%)	4.77×10^{-4} (2.20%)	3.46×10^{-4} (1.60%)

with different lengths are more likely to improve extraction accuracy and bandwidth, which could be optimized further by averaging multiple transmission line groups of comparisons. However, using multiple transmission lines could increase the number of measurements and the complexity of the extraction process. Hence, it requires a trade-off between procedure complexity and extraction accuracy. Our method has realized acceptable accuracy within a certain bandwidth by only utilizing two transmission lines, which could meet some general requirements. The proposed two-line algorithm is not only suitable for the dielectric extraction of UGCPW straight-line structures, but also other types of transmission lines. By obtaining the ABCD parameters from measured S-parameters, and then separating various losses under the corresponding structures and dimensions, the dielectric property is expected to be achieved. Due to the difference of structures and electric field distributions of various types of transmission lines, the calculation formula and separation algorithm of conductor loss/radiation loss would be different, and a systematic comparison of the extraction algorithm is required.

IV. CONCLUSION

A novel two-transmission-line method based on an optimized ABCD matrix has been proposed for dielectric characterization of substrate materials in a broad and continuous frequency band. Both of the single-line and two-line algorithms have been discussed based on UGCPW configuration, which is very suitable for electroplating circuits with a consistent conductor layer on newly developed substrates. The experimental results show that the extraction parameters based on the two-line algorithm match the reference values better than that of the single-line algorithm. The influence of fabrication tolerance and VNA measurement error for the extracted results has been analyzed, and the uncertainty budgets at selected frequencies are presented. The proposed method with high extraction accuracy is expected to be applied to any transmission lines with arbitrary characteristic impedance, without a prior knowledge of substrate dielectric constant and additional calibrations other than the calibration for measurement setup (VNA).

ACKNOWLEDGMENT

The authors would like to thank R. Mei for the help of manuscript proofreading.

REFERENCES

[1] F. Declercq, H. Rogier, and C. Hertleer, "Permittivity and loss tangent characterization for garment antennas based on a new matrix-pencil two-line method," *IEEE Trans. Antennas Propag.*, vol. 56, no. 8, pp. 2548–2554, Aug. 2008.

[2] S. Sahin, N. K. Nahar, and K. Sertel, "Permittivity and loss characterization of SUEX epoxy films for mmW and THz applications," *IEEE Trans. THz Sci. Technol.*, vol. 8, no. 4, pp. 397–402, Jul. 2018.

[3] N. Ghalichechian and K. Sertel, "Permittivity and loss characterization of SU-8 films for mmW and terahertz applications," *IEEE Antennas Wireless Propag. Lett.*, vol. 14, pp. 723–726, 2015.

[4] I. Maestrojuan, I. Palacios, I. Ederra, and R. Gonzalo, "USE of COC substrates for millimeter-wave devices," *Microw. Opt. Technol. Lett.*, vol. 57, no. 2, pp. 371–377, Feb. 2015.

[5] L. Cai, Z. Jiang, and W. Hong, "Low-loss substrate material for millimeter-wave and THz applications (invited)," in *Proc. IEEE Int. Symp. Radio-Freq. Integr. Technol. (RFIT)*, Aug. 2019, pp. 1–3.

[6] R. Kumar, P. Kumar, N. Gupta, and R. Dubey, "Experimental investigations of wearable antenna on flexible perforated plastic substrate," *Microw. Opt. Technol. Lett.*, vol. 59, no. 2, pp. 265–270, Feb. 2017.

[7] A. A. Takach, F. M. Moukanda, F. Ndagijimana, M. Al-Husseini, and J. Jomaah, "Two-line technique for dielectric material characterization with application in 3D-printing filament electrical parameters extraction," *Prog. Electromagn. Res. M*, vol. 85, pp. 195–207, Oct. 2019.

[8] K.-P. Latti, M. Kettunen, J.-P. Strom, and P. Silventoinen, "A review of microstrip T-resonator method in determining the dielectric properties of printed circuit board materials," *IEEE Trans. Instrum. Meas.*, vol. 56, no. 5, pp. 1845–1850, Oct. 2007.

[9] X.-C. Zhu, W. Hong, P.-P. Zhang, Z.-C. Hao, H.-J. Tang, K. Gong, J.-X. Chen, and K. Wu, "Extraction of dielectric and rough conductor loss of printed circuit board using differential method at microwave frequencies," *IEEE Trans. Microw. Theory Techn.*, vol. 63, no. 2, pp. 494–503, Feb. 2015.

[10] D. E. Zelenchuk, V. Fusco, G. Goussetis, A. Mendez, and D. Linton, "Millimeter-wave printed circuit board characterization using substrate integrated waveguide resonators," *IEEE Trans. Microw. Theory Techn.*, vol. 60, no. 10, pp. 3300–3308, Oct. 2012.
[11] C. Wan, B. Nauwelaers, and W. De Raedt, "A simple error correction method for two-port transmission parameter measurement," *IEEE Microw. Guided Wave Lett.*, vol. 8, no. 2, pp. 58–59, Feb. 1998.
[12] N. K. Das, S. M. Voda, and D. M. Pozar, "Two methods for the measurement of substrate dielectric constant," *IEEE Trans. Microw. Theory Techn.*, vol. 35, no. 7, pp. 636–642, Jul. 1987.
[13] M.-Q. Lee and S. Nam, "An accurate broadband measurement of substrate dielectric constant," *IEEE Microw. Guided Wave Lett.*, vol. 6, no. 4, pp. 168–170, Apr. 1996.
[14] A. P. Toda and F. De Flaviis, "60-GHz substrate materials characterization using the covered transmission-line method," *IEEE Trans. Microw. Theory Techn.*, vol. 63, no. 3, pp. 1063–1075, Mar. 2015.
[15] L. Cai, Z. H. Jiang, Y. Huang, and W. Hong, "Ungrounded coplanar waveguide based straight line methods for broadband and continuous dielectric characterization of microwave substrates," *IEEE Access*, vol. 8, pp. 32624–32631, 2020.
[16] X. Lin and B.-C. Seet, "Dielectric characterization at millimeter waves with hybrid microstrip-line method," *IEEE Trans. Instrum. Meas.*, vol. 66, no. 11, pp. 3100–3102, Nov. 2017.
[17] J.-S. Hong, *Microstrip Filters for RF/Microwave Applications*, vol. 235. Hoboken, NJ, USA: Wiley, 2011.
[18] R. E. Collin, *Foundations for Microwave Engineering*. New York, NY, USA: Wiley, 2001.
[19] M. Riaziat, R. Majidi-Ahy, and I.-J. Feng, "Propagation modes and dispersion characteristics of coplanar waveguides," *IEEE Trans. Microw. Theory Techn.*, vol. 38, no. 3, pp. 245–251, Mar. 1990.
[20] J. Carroll, M. Li, and K. Chang, "New technique to measure transmission line attenuation," *IEEE Trans. Microw. Theory Techn.*, vol. 43, no. 1, pp. 219–222, Jan. 1995.
[21] P. Seiler and D. Plettemeier, "A method for substrate permittivity and dielectric loss characterization up to subterahertz frequencies," *IEEE Trans. Microw. Theory Techn.*, vol. 67, no. 4, pp. 1640–1651, Apr. 2019.
[22] E. L. Holzman, "Wideband measurement of the dielectric constant of an FR4 substrate using a parallel-coupled microstrip resonator," *IEEE Trans. Microw. Theory Techn.*, vol. 54, no. 7, pp. 3127–3130, Jul. 2006.
[23] A. Kazemipour, M. Wollensack, J. Hoffmann, M. Hudlička, S.-K. Yee, J. Rüfenacht, D. Stalder, G. Gäumann, and M. Zeier, "Analytical uncertainty evaluation of material parameter measurements at THz frequencies," *J. Infr., Millim., THz Waves*, vol. 41, no. 10, pp. 1199–1217, Oct. 2020.
[24] N. Shoaib, *Vector Network Analyzer (VNA) Measurements and Uncertainty Assessment*. Cham, Switzerland: Springer, 2017.
[25] H. B. Wang and Y. J. Cheng, "Broadband printed-circuit-board characterization using multimode substrate-integrated-waveguide resonator," *IEEE Trans. Microw. Theory Techn.*, vol. 65, no. 6, pp. 2145–2152, Jun. 2017.
[26] N. Shoaib, M. Sellone, L. Brunetti, and L. Oberto, "Uncertainty analysis for material measurements using the vector network analyzer," *Microw. Opt. Technol. Lett.*, vol. 58, no. 8, pp. 1841–1844, Aug. 2016.
[27] M. Wollensack, J. Hoffmann, J. Ruefenacht, and M. Zeier, "VNA tools II: S-parameter uncertainty calculation," in *Proc. 79th ARFTG Microw. Meas. Conf.*, Jun. 2012, pp. 1–5.
[28] M. Zeier, J. Hoffmann, and M. Wollensack, "Metas. UncLib—A measurement uncertainty calculator for advanced problems," *Metrologia*, vol. 49, no. 6, p. 809, 2012.

LONGZHU CAI (Member, IEEE) received the B.Eng. degree from the Huazhong University of Science and Technology, Wuhan, China, and the University of Birmingham, Birmingham, U.K., in 2012, and the M.Res. and Ph.D. degrees from the University of Cambridge, Cambridge, U.K., in 2013 and 2017, respectively.

In 2017, he joined the School of Information Science and Engineering, Southeast University, Nanjing, China. His current research interests include microwave (MW) component designs, study of smart materials, and the development of liquid crystal as a tunable dielectric for MW applications.

ZHI HAO JIANG (Member, IEEE) was born in Nanjing, China, in 1986. He received the B.S. degree in radio engineering from Southeast University, Nanjing, in 2008, and the Ph.D. degree in electrical engineering from The Pennsylvania State University, University Park, State College, PA, USA, in 2013.

From 2013 to 2016, he was a Postdoctoral Fellow with the Computational Electromagnetics and Antennas Research Laboratory, Department of Electrical Engineering, The Pennsylvania State University. He is currently a Professor with the State Key Laboratory of Millimeter Waves, School of Information Science and Engineering, Southeast University. He has authored or coauthored about 80 articles in peer-reviewed journals, over 70 articles in conference proceedings, as well as eight book chapters. He has also co-edited one book: *Electromagnetics of Body-Area Networks: Antennas, Propagation, and RF Systems* (Wiley/IEEE Press, 2016). He holds seven granted U.S. patents and one granted Chinese patent. He serves as a reviewer for more than 40 journals. His current research interests include microwave/millimeter-wave antennas and circuits, millimeter-wave systems, impedance surfaces, metamaterials, and analytical methods. He has served as the TPC Co-Chair or a TPC member for multiple international conferences. He was a recipient of the Young Scientist Award at the 2019 ACES-China Conference, the High-Level Innovative and Entrepreneurial Talent presented by Jiangsu Province, China, in 2017, the Thousands of Young Talents presented by China Government in 2016, the Honorable Mention in 2013 IEEE AP-S International Symposium on Antennas and Propagation Student Paper Contest, and the 2012 A. J. Ferraro Outstanding Doctoral Research Award in Electromagnetics. He also serves as the Associate Editor for *IET Communications*. He was a Guest Editor of *International Journal of RF and Microwave Computer-Aided Engineering*.

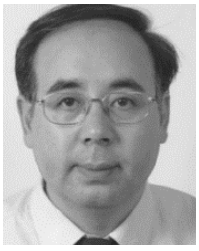

WEI HONG (Fellow, IEEE) received the B.S. degree in radio engineering from the University of Information Engineering, Zhengzhou, China, in 1982, and the M.S. and Ph.D. degrees in radio engineering from Southeast University, Nanjing, China, in 1985 and 1988, respectively.

In 1993, he joined the University of California at Berkeley, Berkeley, CA, USA, as a short-term Visiting Scholar. From 1995 to 1998, he was a short-term Visiting Scholar with the University of California at Santa Cruz, Santa Cruz, CA, USA. Since 1988, he has been with the State Key Laboratory of Millimeter Waves, Southeast University, where he has been the Director since 2003. He is currently a Professor and the Dean of the School of Information Science and Engineering. He is involved in numerical methods for electromagnetic problems, millimeter-wave theory and technology, antennas, and RF technology for wireless communications. He has authored or coauthored over 300 technical publications with over 9000 citations and has authored two books. He is also a Fellow of CIE. He was twice awarded the National Natural Prizes and thrice awarded the first-class Science and Technology Progress Prizes issued by the Ministry of Education of China and Jiangsu Province Government. He also received the Foundations for China Distinguished Young Investigators and for "Innovation Group" issued by NSF of China. He was an Elected IEEE MTT-S Ad Com Member from 2014 to 2016. He is also a Vice President of the CIE Microwave Society and Antenna Society and the Chair of the IEEE MTT-S/AP-S/EMC-S Joint Nanjing Chapter. He has served as an Associate Editor for the IEEE TRANSACTIONS ON MICROWAVE THEORY AND TECHNIQUES from 2007 to 2010. He was one of the guest editors of the 5G Special Issue of the IEEE TRANSACTIONS ON ANTENNAS AND PROPAGATION in 2017.